Pergamon

Deep-Sea Research I, Vol. 44, No. 9–10, pp. 1467–1495, 1997

PII: S0967–0637(97)00016–2
0967–0637/97 $17.00 + 0.00

Circulation off Algeria inferred from the Médiprod-5 current meters

CLAUDE MILLOT,*† MEJDOUB BENZOHRA* and ISABELLE TAUPIER-LETAGE*

(*Received* 24 *July* 1995; *in revised form* 1 *July* 1996; *accepted* 13 *January* 1997)

Abstract—Eight moorings were deployed off Algeria (1–5°E) during the Médiprod-5 experiment (June 1986–March 1987). The 24 current meter time series recorded at nominal depths of 100, 300, 1000 and 2000 m are analysed together with hydrological data (May–June 1986) and satellite infra-red images. As expected, the circulation features are markedly different inside and outside of a ~50 km-wide coastal zone. At ~25 km from the coast, five out of six moorings are well within the Algerian Current and the current profile is strongly sheared, with low correlations at depth. All water masses flow eastward along the Algerian slope, thus completing consistently our circulation diagrams. At ~75 km, the currents are more correlated between 300 and 2000 m and more dependent on the occurrence of mesoscale (100-200 km) anticyclonic eddies called "open sea eddies".

An event was recorded, propagating eastward at ~3 km/day across the mooring array. It is thought to consist of a meander (width 50–150 km) of the Algerian Current, extending to ~100 km from the coast and associated with two superimposed anticyclonic eddies. One eddy, enclosed within the meander, involved the surface layer and had the infra-red signature of what we previously called a "coastal eddy" (30–120 km apparent diameter). The other eddy seemingly involved the whole deep layer, rapidly became barotropic and large in diameter (up to ~150 km) which made it coastal too. Sooner or later, both coastal eddies are expected to merge together.

These measurements have slightly modified our former hypotheses as, instead of assuming that "open sea eddies" are old stages of coastal surface eddies becoming larger and deeper, we now expect them to be old stages of the merged coastal eddies. This new understanding of such a coastal event is more similar to an open sea eddy and seems consistent with both theoretical models and laboratory experiments. Whatever this structure, recent data support our former hypotheses that mesoscale eddies generated by the Algerian Current can have a deep extent, propagate along the Algerian and then Sardinian slopes (where they entrap Levantine Intermediate Water) and strongly influence the circulation of all water masses. © 1997 Elsevier Science Ltd

1. INTRODUCTION

In the Mediterranean, evaporation exceeds precipitation and river runoff, thus creating a 1–2 Sv inflow through the Strait of Gibraltar. As this flow proceeds eastward, its characteristics change and it is recognized everywhere as a 150–200 m layer of Modified Atlantic Water (MAW). Within the Alboran Sea, it generally describes two anticyclonic gyres, but only the western one can be considered as quasi permanent. When the eastern gyre is present, it is associated with a jet crossing the sea, from the vicinity of Almeria, Spain to that of Oran, Algeria. Otherwise, the circulation in the eastern Alboran Sea is generally eastward along the African coast (Parrilla and Kinder, 1987) or more complex (Millot, 1987a).

*Centre d'Océanologie de Marseille, Antenne de Toulon CNRS URA 41, BP 330, F-83507 La Seyne, France.
†Author to whom correspondence should be addressed.

In the Algerian Basin, the general circulation features are more debated. Basically, historical diagrams (e.g. Ovchinnikov, 1966) as well as recent numerical models (e.g. Roussenov *et al.*, 1995) depict a permanent "branching" of the MAW flow, one branch flowing eastward via the Channel of Sardinia and the other north-eastward. About 10 years ago, such a branching was refuted by Millot (1985, 1987a), who assigned a major role to the mesoscale. Briefly, it was argued that the MAW flow along the Algerian slope, which has been named the Algerian Current, has a wedge-shaped structure. This current is baroclinically unstable and often forms meanders enclosing surface anticyclonic eddies (50–100 km) propagating eastward at a few km/day, sometimes for months. An upwelling is generated where the upstream part of the meander leaves the coast, and the cold and chlorophyll-richer water is entrained along the inner side of the meander, thus acting as a tracer for the satellite thermal and visible detection of the eddy it encloses. It was formerly hypothesized that some of these coastal surface eddies could increase their diameter (up to 100–200 km) and depth (up to more than ~ 1000 m) during their eastward course, and leave the coast at some point, thus becoming what we called "open sea eddies". In the light of the observations about event "E" presented hereafter, a meander and the surface eddy it encloses could be associated with another type of coastal eddy, rapidly arising wide and deep below the MAW layer, the merging and drifting seaward of both coastal eddies then leading to an open sea eddy.

Whatever the connections between these eddies, open sea eddies are determinant for the circulation in the Algerian Basin. If they come back close to the coast, they can dramatically interact with the Algerian Current, which then flows seaward for months, as "W" in 1984 (Taupier-Letage and Millot, 1988) and "O" in 1986 (Millot, 1991; Benzohra and Millot, 1995a,b, hereafter BMa,b). They can be motionless (as "O") or not, as the ~ 100-km eddy ("O'" in Fig. 1 of BMa) clearly followed on infra-red images in May–June 1986 drifting westward at ~ 3 km/day. Thus, we still object to the concept of a quasi permanent "branching" of the MAW flow and favour occasional dispatching, due to the generation of, and/or interaction with, mesoscale anticyclonic eddies.

A similar controversy exists for the circulation of the warm-salty Levantine Intermediate Water (LIW) which enters the Algerian Basin through the Channel of Sardinia and flows at 200–600 m. Basically, the same historical papers (as well as recent ones, e.g. Haines and Wu, 1996) depict a "branching" of LIW, one branch flowing cyclonically in the interior of the sea (roughly between France and Algeria), and the second flowing westward off Algeria, directly toward the Strait of Gibraltar. Herbaut *et al.* (1996) also depict a branching, but with the former vein flowing along the Sardinian continental slope. On the contrary, Millot (1987a,b) refutes any "branching" and depicts a unique LIW vein, flowing cyclonically along the continental slope, which can be eroded by eddies near Sardinia and thus be dispatched as lenses or patches in the interior of the Algerian Basin. Other papers have provided complementary information supporting the non-occurrence of a westward branch off Algeria (Katz, 1972), the importance of the mesoscale eddies there (Burkov *et al.*, 1979), and the occurrence of a LIW vein along the Sardinian slope (Perkins and Pistek, 1990). Therefore, even the mean path of LIW is still debated.

It is clear from recent estimations (Harzallah *et al.*, 1993) that MAW and LIW are the most important components of the Mediterranean "conveyor belt". The debate about their circulation features, which does not solely concern the Algerian Basin, is thus representative of our presently poor understanding of the functioning of the sea. Moreover, there are some secondary water masses whose circulation has not yet been depicted. Between MAW and

LIW, one generally encounters Winter Intermediate Water (WIW), which is MAW cooled during the winter in the northern part of the western Mediterranean (Lacombe and Tchernia, 1960; Conan and Millot, 1995), and thus identified by a temperature minimum. When wintery atmospheric interactions are especially intense, MAW and LIW mix and form the Western Mediterranean Deep Water (WMDW), which spreads below ~600 m. More heterogeneous waters (generic name is Bottom Water, BW), which can be found everywhere close to the bottom (Lacombe *et al.*, 1985), are especially dense waters recently formed in the Gulf of Lions. Hopkins (1988) favours a permanent inflow of WMDW into the Tyrrhenian Sea, as if sucked by the mixing with LIW to form the Tyrrhenian Deep Water (TDW). We rather favour an occasional overflow of WMDW from the Algerian Basin, thus assuming that most of the outflow from the Tyrrhenian Sea comes from the Channel of Sicily (LIW and denser waters). In any case, it is difficult to differentiate the water masses at 1000–2000 m from their hydrological characteristics and we will continue to deal with LIW and WMDW only.

About 10 years ago, little was demonstrated definitively about the circulation in the interior of the sea while major questions concerned the Algerian Basin (Millot, 1987a). Therefore we took the opportunity of the Western Mediterranean Circulation Experiment (La Violette, 1990) to conceive the French–Algerian experiment presented in Section 2. The current data are described in Section 3 and statistically analysed in Section 4. Section 5 focuses on the analysis of a specific event ("E") of importance for the understanding of the whole system.

2. THE MÉDIPROD-5 EXPERIMENT

We intended to describe some basic features off Algeria, especially the structure of the MAW flow, i.e. the Algerian Current and the conditions for its stability, the structure of the coastal and open sea eddies and their relationships, the circulation of LIW and, finally, the biological consequences of the mesoscale phenomena. The Médiprod-5 experiment was based on a 1-month campaign (May–June 1986), during which ~100 CTD casts (0–800 db) were collected, 5 drifting buoys (drogued at 10 m) were launched, and 28 current meters were moored at 8 points for more than 9 months. The salient aspect of the campaign is that it was conducted with the determining help of satellite infra-red information received on board in near-real time. Specific mesoscale phenomena were thus efficiently sampled with a few-kilometre spacing.

The paper is based on infra-red images and current and temperature data collected at 0–5°E (Fig. 1), where no current measurements were previously available. Aanderaa RCM4-5 were deployed at nominal depths of 100, 300, 1000 and, at some points, 2000 m. To correctly resolve phenomena ranging from the inertial (~20 h) to the mesoscale while getting several-month records, the sampling interval was set to 1 h. On the basis of our circulation diagrams, a coastal group of six moorings (points 1, 2, 3, 4, 6, 8) was deployed at ~25 km from the coast to describe the Algerian Current and its associated meanders and eddies. An offshore group of two moorings (points 5, 7) was located at ~75 km to describe the circulation in the interior of the basin, expected to be dominated by open sea eddies. The mooring spacing was generally ~100 km, that is, roughly the scale of the phenomena of interest. This coarse resolution was a trade-off between what was required for a detailed study of the eddies and a long-term survey of propagating mesoscale phenomena. To specify the translation speed of the phenomena while in their initial stage, points 1 and 2 were set

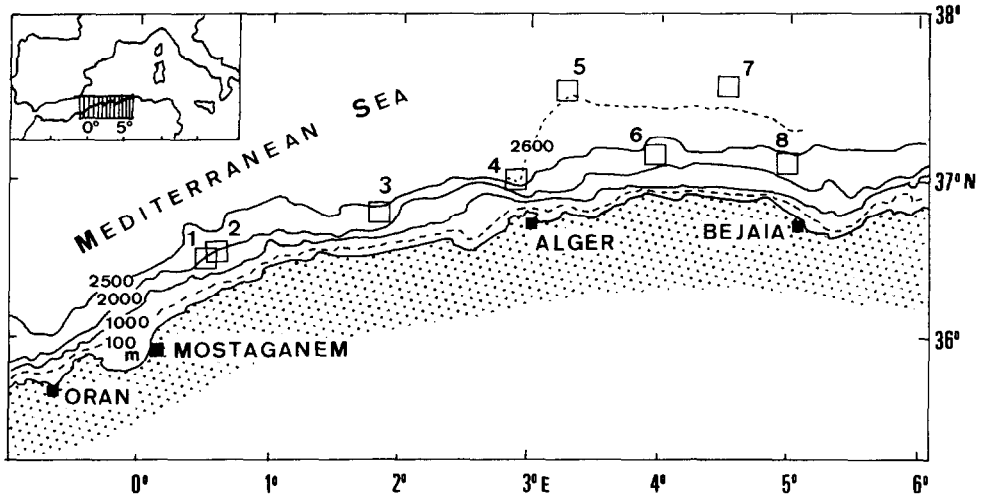

Fig. 1. The Médiprod-5 mooring array.

~ 10 km apart. In the following, each time series/current meter is defined by two numbers, one for the mooring point (1–8) and the other for the immersion (100, 300, 1000 and 2000 m).

Four meters (2–100, 2–300, 4–100, 4–300) were lost. The mooring heads occasionally sank by a few tens of meters while, at depth, maximum sinkings were ~ 10 m. The temperature sensors (resolution 0.025°C) were calibrated before and after the experiment, but the 7–1000 and 7–2000 records are not valid. The 5–100 rotor threshold was abnormally high (speed underestimated). The good quality of the current measurements is demonstrated by the consistent analysis of the M2, S2 and N2 tidal components which, even if somewhere as low as a few mm/s, have been shown to be clearly barotropic and continuously decreasing eastward (Albérola *et al.*, 1995a). The time series were low-passed using a 60 + 1 + 60 Lanczos-cosine filter, with a 40 h half-power point.

During the May–June 1986 campaign, several CTD transects were made across the Algerian Current, especially near 0–1°E (transport ~ 1.7 Sv). We sampled several coastal eddies between ~ 1 and 5°E and an open sea one ("O") centred in the north-east of the mooring array (4°40′E–38°N). Eddy "O" clearly created a cul-de-sac effect, as it interacted with the Algerian Current, which was flowing entirely seaward, during several months, before it could reach ~ 6°E. Some data sets and preliminary analyses have been presented in Millot and Bonin (1990), and the hydrological data have now been completely analysed in several papers. Millot (1987b) focused on the spatial variability of LIW. Our LIW circulation diagram has been completed by depicting LIW as sometimes crossing the Alboran Sea from Spain to Algeria, due to the entrainment of MAW, and then proceeding eastward along the Algerian slope thus flowing cyclonically around most of the western Mediterranean (Millot, 1994). Statistical computations account for MAW and WIW flowing as LIW (eastward along the Algerian slope) before spreading seaward due to interactions with the open sea eddy "O" (BMa). An analysis of eddy "O" is presented in BMb. Some current meter data have already been used by Millot *et al.* (1990) to give a general description of the Algerian eddies. The marked differences at large and meso-

scales between the southern and northern parts of the western Mediterranean have been shown by Millot (1991). Millot (1994) has shown that the current measurements at depth provide definite information on the general circulation of the intermediate and deep water masses.

3. THE OBSERVATIONS

Only the daily current and temperature time series that are of major interest, basically at 100 and 300 m in the coastal zone and at all depths in the offshore one, are plotted in Fig. 2.

3.1. *Currents*

In the coastal zone, the features at 100 m (in the MAW layer) are relatively different from west to east. The 1–100 speeds (Fig. 2a) are generally low because the meter was just out of the Algerian Current. When in the direction of the mean flow, the 3–100 speeds (up to ~ 30 cm/s, Fig. 2c) are larger than the 6–100 (Fig. 2h) and 8–100 (Fig. 2n) speeds, which is due to the horizontal widening, vertical thinning and finally seaward spreading (due to its interaction with "O") of the whole Algerian Current before the passage of "E". Indeed, before that time, "O" was blocking the natural route of the current eastward along the slope. Then, "O" is seen at a more seaward location and can be thought to have been pushed by "E", thus reopening the eastward route to the current. When the 100-m speeds are not in the direction of the mean flow, they are related to the mesoscale and comparable. This accounts for the phenomena generally attaining a relatively mature stage quite early and not evolving much east of point 3. The most intense mesoscale currents appearing on the 100-m stick diagrams are due to event "E", which crossed the array from early July at point 1 to mid-November at point 8, while another intense mesoscale phenomenon crossed only at point 1 in mid-February (Fig. 2a), just before the mooring recovery.

At 300 m, that is in the upper LIW layer (or in the lower MAW layer when it is deep), the currents are weaker than at 100 m, but the major features are similar. Point 1 (Fig. 2b) is out of the main flow, which is intense at point 3 (Fig. 2d) and decreases eastward (Fig. 2i,o). At mesoscale, the amplitudes are relatively large during the passage of "E" at 1–300 and 3–300, during the passage of "E" and two subsequent phenomena at 6–300 (in early and late December), and mainly during the passage of the latter at 8–300 (about 1 month later). Note that this indicates the possibility for mesoscale phenomena to be generated east of 3°E.

At 1000 m, the eastward mean flow is generally significant and the mesoscale variability noticeable ("E" is signed, although differently, at points 1, 2, 6 and 8 but not clearly at points 3 and 4). At 2000 m, the mean currents are clearly eastward, and larger (up to 4 cm/s) than at 1000 m, which has been observed at the foot of the continental slope in other places of the sea, thus accounting for the circulation of WMDW along the topography (Millot, 1994). "E" is clearly signed only at 1–2000, where it is similar to, although larger than at 1–1000.

In the coastal zone, the mesoscale currents at 100 and 300 m due to "E" are visually similar only at point 1. At the other points, the signatures of "E" are either clear at both depths but very different (as at point 3), or clear at 100 m and unclear at 300 m (as at points 6 and 8). There is no visible coherence between 300 and 1000 m while the only significant coherence between 1000 and 2000 m is at point 1. Thus, the overall idea arises that, if point 1 is excluded because mainly located out of the Algerian Current, "E" and the mesoscale phenomena in general are markedly baroclinic in the coastal zone.

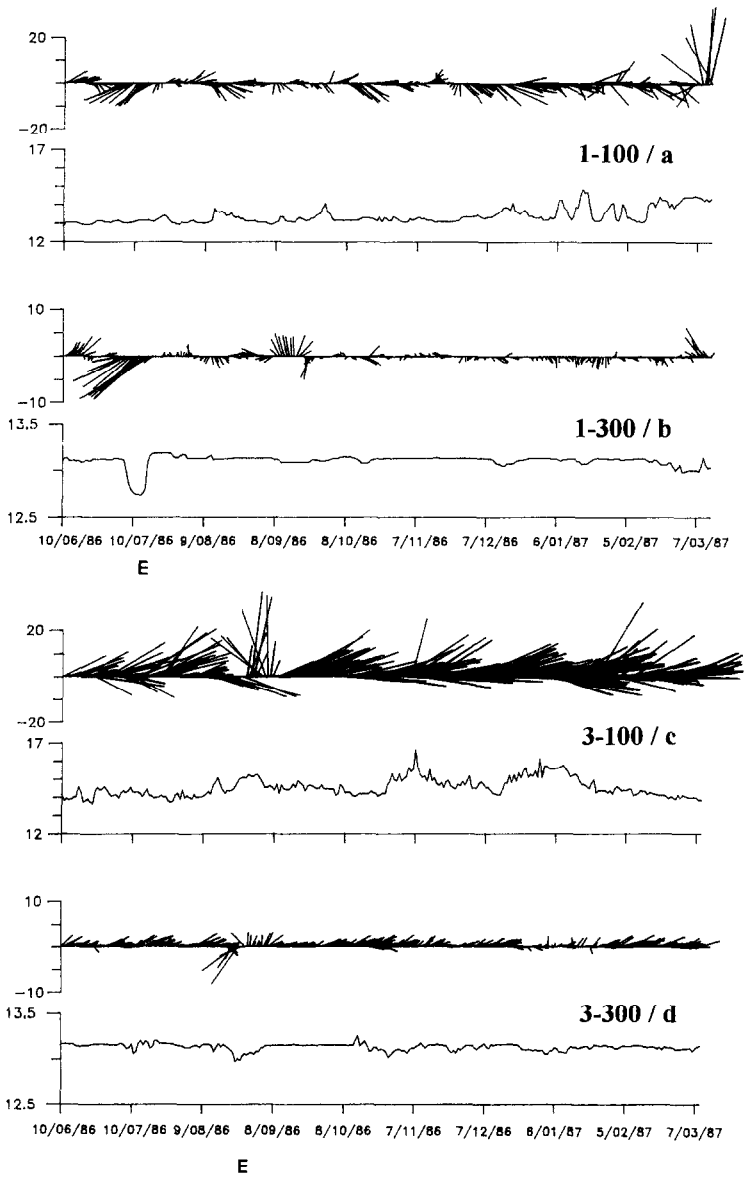

Fig. 2. Current stick diagrams (cm/s; north upward) and temperature (°C) records. The signature of the specific event "E" is indicated.

In the offshore zone, mainly filled by eddies, the circulation is neither quiet nor smooth, as demonstrated by the intense mesoscale fluctuations at points 5 (Fig. 2e–g) and 7 (Fig. 2j–m). Even if the 5–100 speed is underestimated, "E" and two other mesoscale phenomena are clearly signed at 100 m and, although differently, also at 300 and 1000 m. Speeds as large as in the coastal zone have been measured at 7–100, which will be shown to result from the

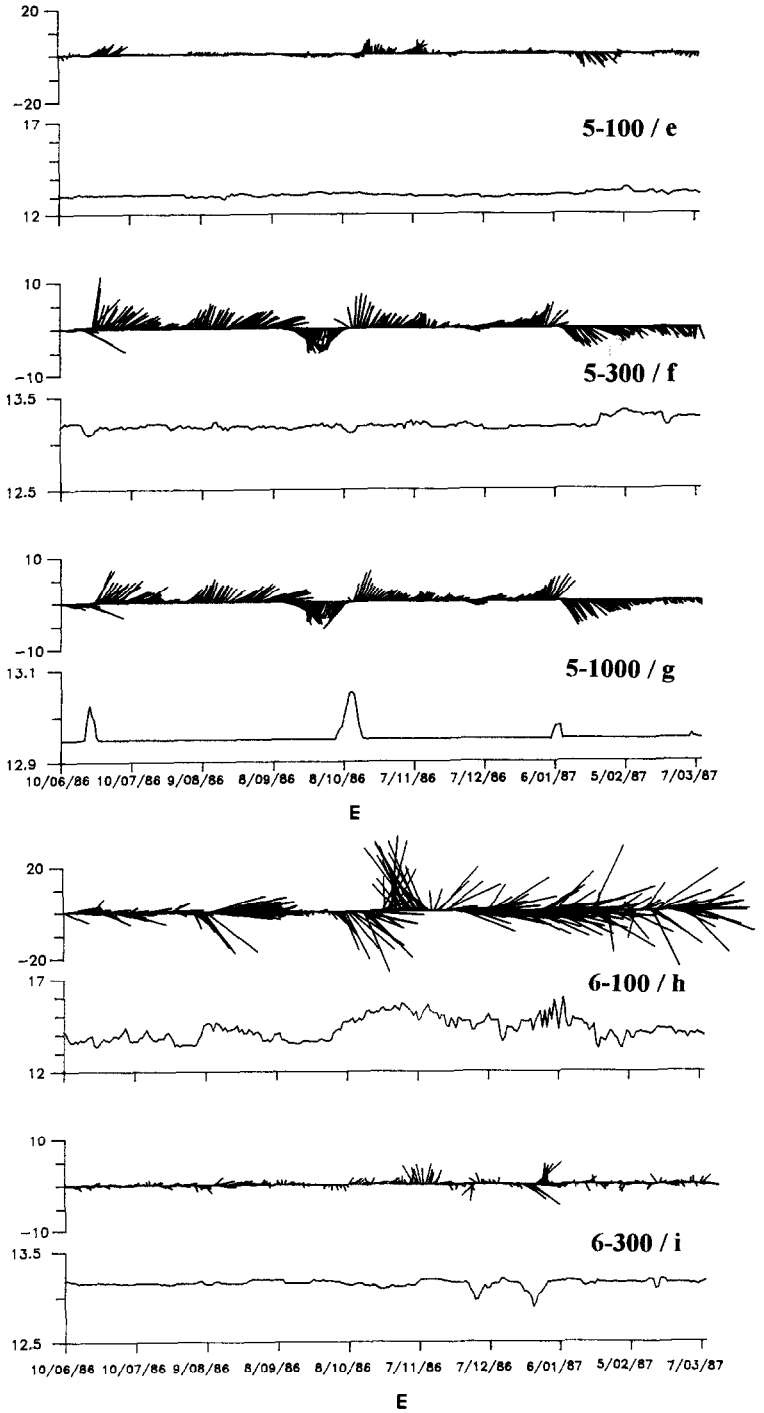

Fig. 2. (*continued*)

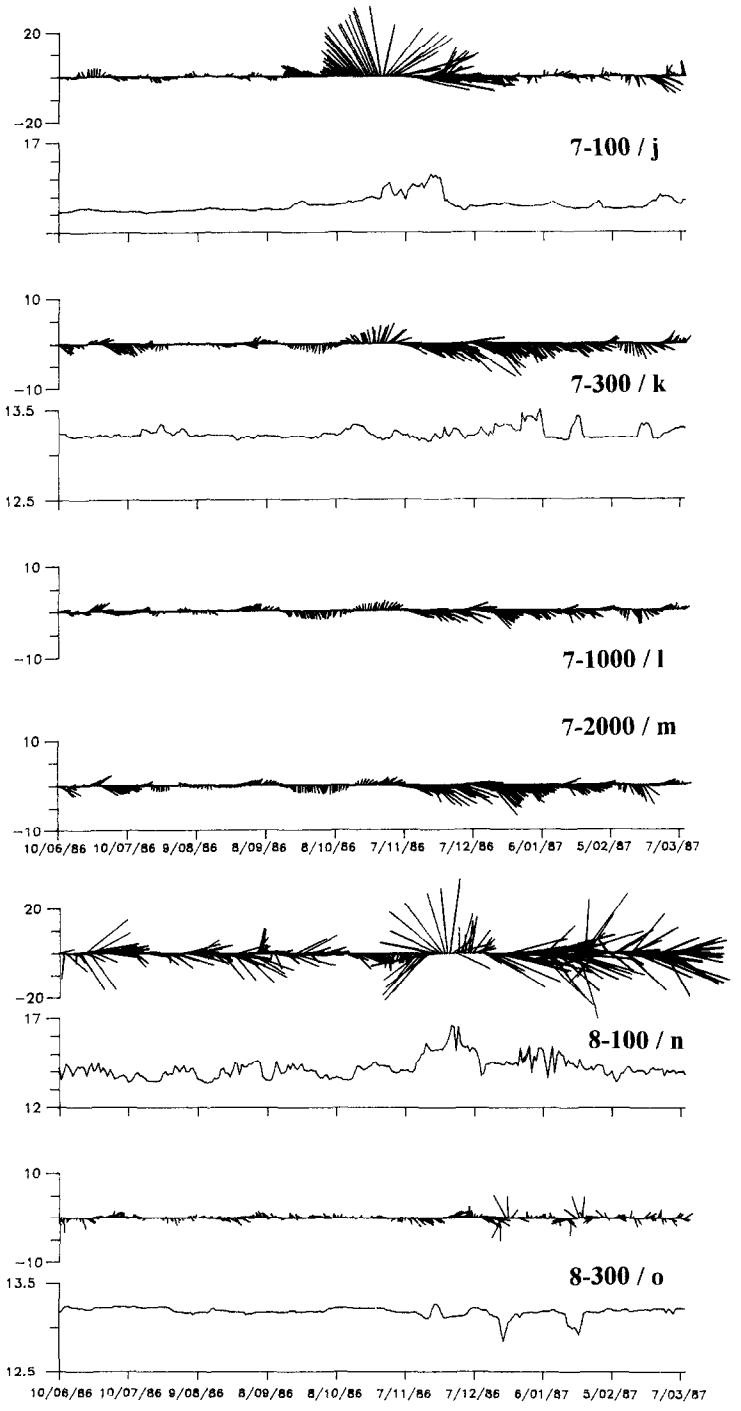

Fig. 2. (*continued*)

interaction between "E" and "O". A striking feature of the offshore zone is that most of the mesoscale phenomena appear to be very similar between ~300 and 2000 m.

Therefore, the major visible differences between the two zones consist of both mesoscale phenomena and mean currents being, below the MAW layer, mainly baroclinic in the coastal zone and barotropic in the offshore one.

3.2. *Temperature*

Most of the mesoscale temperature variations can be explained by vertical displacements of the isotherms, i.e. mainly subsidence induced by anticyclonic motions. It must be kept in mind that the mean potential temperature decreases down to 150–200 m (WIW core), then increases down to 300–400 m (LIW core) and decreases again down to more than ~2000 m (through WMDW) while the *in situ* temperature continuously increases below ~1500 m. In the surface layer, variations also occur at larger scales, while major differences between the points are due to their location with respect to the wedge-shaped Algerian Current. At intermediate depths, the very different characteristics of LIW in the coastal and offshore zones (Millot, 1987b) must be taken into account. On all records, few-day variations are superimposed to mesoscale (tens of days) variations, the latter being generally associated with the phenomena we are interested in.

In the coastal zone, the variations are complex. At 1–100 (Fig. 2a), at the entrance of the Algerian Basin, where mesoscale phenomena are generally not mature, "E" is not clearly signed. At 3–100 (Fig. 2c), the increase due to "E" depressing the MAW layer can be seen, but larger fluctuations are not clearly associated with current fluctuations. More classic temperature–current relationships are observed at 6–100 (Fig. 2h) and 8–100 (Fig. 2n), where the highest temperatures are due to "E". At 300 m, most of the variations are troughs linked to the subsidence of the WIW layer by anticyclonic motions. At 1–300 (Fig. 2b), both "E" and the February phenomenon induced deep troughs, the former leading to the lowest recorded value (~12.70°C). "E" is also clearly signed at 3–300 (Fig. 2d), and to a lesser extent at 6–300 (Fig. 2i). Its signature at 8–300 (a maximum between two minima, Fig. 2o) is certainly due to a large subsidence, depressing not only WIW but also the warmer MAW down to 300 m. The delay between the troughs at 6–300 and 8–300 due to the two phenomena subsequent to "E" corresponds to a few-km/day eastward translation speed. At greater depths, the natural variability is of the order of the instruments resolution (0.025°C), but the mean temperatures are consistent with the historical temperatures (Guibout, 1987; Picco, 1990; Brasseur *et al.*, 1993). At 1000 m, the temperature displays small peaks that cannot be clearly related either to current variations or to temperature variations at the upper levels. For instance, "E" is signed at all points but at 6–1000, while the two subsequent phenomena are signed more clearly at 8–1000 than at 6–1000. At 2000 m, the sole mesoscale fluctuations that appear consistent with those at upper levels are associated with "E" at 8–2000.

In the offshore zone, and due to the wedge-shaped section of the Algerian Current, the mean temperatures at 100 m are lower than in the coastal zone by ~1°C (Fig. 2e,j). At mesoscale, the only clear variation is due to "E" at 7–100. At 300 m (Fig. 2f,k), unlike in the coastal zone, both troughs and peaks are observed. Two examples of troughs, due to a deepening of WIW, occur at 5–300 in late June and early October (due to "E"). But peaks are more frequent, in agreement with our hypothesis that the more recent–warmer LIW is distributed as lenses or patches in the interior of the Algerian Basin while the older–cooler

water is found along the Algerian slope. This is supported by the CTD data of the May–June campaign (Millot, 1987b, 1994; BMa,b), and by XBT data recently collected between France and Algeria (Fuda and Millot, 1995). At 1000 m, peaks sometimes reaching 0.1°C appear on the sole available record (5–1000, Fig. 2g). Such a large amplitude also supports the presence of relatively recent LIW in the whole offshore zone. At least the first and second (due to "E") peaks at 1000 m are associated with troughs at 300 m, which indicates that subsidence is perceptible over large depth intervals. On the basis of the scarce available hydrological data, the subsidence induced near 5–1000 by "E" is 250–300 m, a value similar to the one induced by "O" (BMb). Note that the peaks at 5–300 and 5–1000 are associated with marked and similar rotations of the current, meaning that "E" and the mesoscale phenomena in general induce large and coherent anticyclonic motions over most of the deeper layer.

4. BASIC STATISTICS

The means and standard deviations of the temperature (T, σ_T) and of the along-shore (U, σ_U) and cross-shore (V, σ_V) current components have been computed with 95% error intervals (Table 1). As the inertial frequency has been filtered out, the variance is mainly

Table 1. *Basic statistics*

Point	z (m)	U (cm/s)	σ_u (cm/s)	V (cm/s)	σ_v (cm/s)	Θ* (°)	e**	τ_u (days)	τ_v (days)	T (°C)	σ_T (°C)	τ_T (days)
1[1]	100	4.6±2.1	7.0	−2.5±1.7	7.2	−51	0.5	6	4	13.39±0.19	0.428	13
	300	−0.4±0.9	2.4	−0.3±0.7	2.1	37	0.9	9	7	13.10±0.02	0.067	6
	1000	−0.1±0.9	1.2	0.2±0.2	0.9	−15	0.8	6	3	12.95±0.00	0.012	8
	2000	1.1±0.9	2.8	0.3±0.2	1.0	−9	0.9	7	3	13.10±0.00	0.007	16
2[1]	1000	0.6±0.4	1.7	−0.0±0.2	1.1	−17	0.8	4	3	12.95±0.00	0.006	4
3	100	23.1±3.0	10.2	4.5±1.8	8.6	−20	0.6	6	3	12.94±0.00	0.511	12
	300	2.6±0.5	1.7	0.8±0.2	1.1	26	0.9	5	3	14.52±0.21	0.036	6
	1000	1.2±0.4	1.5	0.2±0.6	1.3	34	0.8	6	12	13.13±0.01	0.007	8
4	1000	1.7±0.4	0.9	0.1±0.1	0.4	−6	0.9	14	3	12.95±0.00	0.022	37
	2000	4.2±1.0	2.2	−0.4±0.5	1.2	−10	0.9	19	16	12.94±0.01	0.004	5
5	100	1.2±0.4	1.6	0.3±0.7	1.9	77	0.6	5	10	13.08±0.00	0.092	14
	300	2.7±0.9	2.1	0.7±1.2	3.0	78	0.7	12	11	13.07±0.04	0.047	14
	1000	2.7±1.0	2.1	0.5±1.0	2.7	65	0.7	15	10	13.19±0.02	0.014	5
6	100	11.9±3.7	10.1	0.7±2.7	9.2	−37	0.7	9	6	12.95±0.00	0.587	16
	300	0.7±0.4	1.3	0.2±0.3	1.2	−22	0.4	5	3	14.24±0.29	0.042	6
	1000	1.0±0.4	1.4	0.1±0.2	0.9	−14	0.8	6	4	12.95±0.00	0.007	8
7	100	2.7±4.2	8.6	1.6±2.6	6.7	−26	0.8	16	10	13.50±0.23	0.429	19
	300	2.2±1.3	2.6	−1.0±0.7	1.9	−28	0.8	17	11	13.23±0.02	0.061	6
	1000	1.7±0.8	1.6	−0.5±0.4	1.2	−20	0.7	17	7			
	2000	2.3±1.2	2.2	−0.9±0.5	1.5	−24	0.8	20	7			
8	100	9.2±4.4	11.5	−1.0±0.7	8.3	−8	0.7	10	3	14.21±0.25	0.581	13
	300	0.3±0.4	1.4	−0.0±0.3	1.2	−20	0.6	5	3	13.17±0.02	0.052	7
	1000	0.8±0.4	1.2	0.2±0.2	0.8	−27	0.9	7	3	12.95±0.00	0.002	4
	2000									13.08±0.01	0.009	50

*The principal axis direction (Θ) is measured anticlockwise from east.

**e is the variance ellipse eccentricity.

[1]The current vector is projected on an axis oriented 30° anticlockwise from east.

indicative of the mesoscale. The along-shore component is positive eastward (90°T), except for points 1 and 2 (60°T). The 95% intervals are based on an effective number of degrees of freedom (N) equal to the ratio of the total record length (L) to the integral time scale τ, τ being defined as twice the integrated autocorrelation function computed with a maximum lag of 0.2 L (Davis, 1976). τ is also used to compute correlation confidence levels defined as the inverse of the square root of N multiplied by 1.6, 2.0 or 2.6 to get the 90%, 95% or 99% levels, respectively (Sciremammano, 1979). The values of the principal axis orientation (Θ) and the eccentricity (e) of the variance ellipses are reported in Table 1; the mean currents and the variance ellipses are drawn in Fig. 3.

4.1. *Means and variances*

At all points, the U means are positive, except those at 1–300 and 1–1000, which are negative but non-significant, so that the net 9-month transports of all water masses were eastward. The mean directions are roughly similar over the whole depth and generally parallel to the local isobaths as no open sea eddy like "O" remained over a mooring. Nevertheless, there are clear differences between the two zones. In the coastal zone except point 1, which was out of the Algerian Current, the U means at 100 m are much larger than the V means, and they significantly decrease eastward. This is clearly due to the horizontal widening and vertical thinning of the current, as well as to its spreading seaward around "O" before reaching ~6°E during most of the experiment. The latter mechanism led to the U and V means at 6–300 and 8–300 having similar characteristics. Values at 100 m are about 10 times larger than at 300 m, no general trend is observed between 300 and 1000 m, and U means at 1000 m are lower than the means at 2000 m by ~1 cm/s. This latter feature has also been observed in other places of the sea (Millot, 1994) and accounts for a significant circulation of WMDW cyclonically along the foot of the continental slope. In the offshore zone, including point 1, U and V means are similar and U means are lower than in the coastal zone. Due to the deficient 5–100 rotor and to the strong, even if temporary, influence of "E" at 7–100, the 100-m means cannot be significantly compared with those in the coastal zone. Means at 300 and 1000 m in the offshore zone are larger than in the coastal zone, and are roughly similar at 2000 m. A specific feature of the offshore zone is that values at 300, 1000 and 2000 m are nearly the same at all points.

At 100 m (Fig. 3a), the lowest current variance is at 1–100, which is consistent with the location of point 1 out of the main flow and suggests that mesoscale phenomena attain a relatively large amplitude mainly eastward from 0 to 1°E. Now, the similarity of the 3–100, 6–100 and 8–100 variances is not consistent with our working hypothesis that mesoscale eddies continuously increase in size and intensity while progressing eastward. This similarity accounts for phenomena attaining their mature stage rapidly (e.g. before reaching ~2°E for "E") or for a rough equivalence between those disappearing while progressing eastward (as the one sampled at 4°E in June, BMa) or appearing (as the phenomena subsequent to "E"). The specific orientation of the ellipses with respect to the mean direction at 1–100, 3–100 and 6–100 is due to "E", which induced strong currents directed south-east and then north-west; actually, the major axes are parallel to the mean directions when the 1-month parts of the records most influenced by "E" are removed. At the other points (5, 7 and 8), the currents due to "E" are either roughly parallel or perpendicular to the mean direction, so that the orientation and eccentricity of the ellipses are not modified by "E". Therefore, the mesoscale variability generally occurred in the direction of the mean current, which is not a trivial

observation as, within the Northern Current, it can be parallel in summer (Sammari *et al.*, 1995) and perpendicular in winter (Albérola *et al.*, 1995b).

At 300 m (Fig. 3b) and 1000 m (Fig. 3c) in the coastal zone, the variance does not increase from west to east either. This is also not consistent with the hypothesis that mesoscale

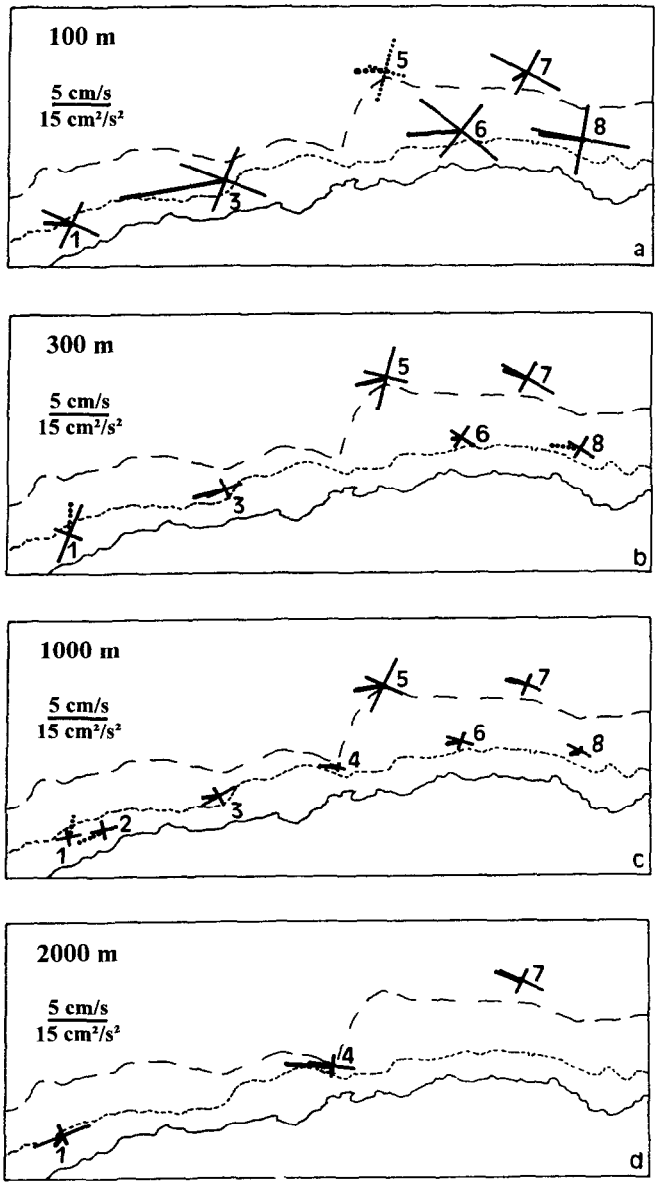

Fig. 3. Mean currents (heavy line) and variance ellipse axes (light line) at 100 m (a), 300 m (b), 1000 m (c) and 2000 m (d), drawn with dotted line if not significant. The mean current vector points to the centre of the ellipse. 2000 m (2600 m) isobath in dotted (dashed) line.

phenomena become deeper while progressing eastward. The large amplitude and specific orientation of the ellipse at 1–300 is clearly due to "E", while the similarity of the ellipses at 300 m at points 3, 6 and 8 agrees with that at 100 m and is interpreted in the same way. The variance at 300 and 1000 m in the offshore zone, especially at point 5, is relatively large. At 2000 m (Fig. 3d), the variance in both zones increases with respect to that at 1000 m. At these depths, the currents due to "E" are either small or not basically different from those induced by the other mesoscale phenomena, so that the direction of the major axes are roughly similar over the whole depth and parallel to the local isobaths. Therefore, the mean values and the ellipses characteristics at 300, 1000 and 2000 m in the offshore (coastal) zone are relatively similar (different), which accounts for both mean and mesoscale currents rather barotropic (baroclinic) over this depth interval.

Temperature means and variances show that the 3–100, 6–100 and 8–100 meters were well within the relatively warm Algerian Current. The slight decrease between 3–100 and the pair 6–100, 8–100 is due to the eastward thinning of the current while lower means at 1–100, 5–100 and 7–100 are in agreement with its wedge-shaped section. Nothing can be deduced from the eastward and shoreward increase of the variance as local gradients must be precisely taken into account. At 300 m, the means increase eastward in both the coastal and the offshore zones, the highest values being at 5–300 and 7–300. Similarly, and not considering 1–300 which is strongly influenced by "E", the variance increases both eastward and seaward. Such a distribution of the mean and variance values at 300 m is consistent with the analysis of the currents and the May–June hydrological data, and supports our hypothesis: relatively mixed–cool LIW flowing eastward in the coastal zone interacts with relatively unmixed–warm LIW issued from the Sardinian vein and dispatched in the offshore zone by eddies. As a result, the mean and the variance at 300 m increase both eastward and seaward in most of the Algerian Basin. At 1000 and 2000 m, the relative homogeneity of the means is noteworthy, which attests to both the reliability of the sensors and the accuracy of the calibration (the ~ 0.13°C increase from 1000 to 2000 m is due to the pressure effect).

4.2. *Time scales*

In both the coastal and the offshore zones, the U time scales are larger than the V time scales. Exceptions are 3–1000, due to a relatively long period of southward current, 5–100, due to relatively long periods of zero speeds, and 4–1000 and 4–2000, as the steep bottom slope near point 4 reduces the amplitude of the fluctuations and leads to relatively large time scales. Both τ_U and τ_V in the offshore zone are significantly larger than in the coastal zone, which could account for phenomena being generally of smaller space scale and/or propagating more rapidly in this latter zone (it will be argued that the first reason is more probable than the second). At 100 m in the coastal zone, τ_U increases eastward, accounting for translation speeds decreasing or space scale increasing eastward. Due to the cul-de-sac effect induced by "O" during most of the experiment, and the fact that the apparent dimension of "E" did not continuously increase while translating eastward (see below), the first reason must be retained.

The temperature time scales do not display marked differences between the coastal and the offshore zones. In general, the τ_T at 100 m are large because the major fluctuations are linked to relatively long-lasting mesoscale phenomena such as "E". The τ_T at 300 and 1000 m are lower because, most of the fluctuations being due to the relative heterogeneity of

the field, they occur during relatively short periods. Due to the poor temperature resolution of the instruments (a fluctuation lower than the resolution leads to values either constant or oscillating between two numerical counts), the τ_T at 2000 m are not significant.

4.3. *Horizontal scales*

Information about the horizontal scales is inferred from correlation coefficients computed between meters at the same depth, assuming isotropy and using autocorrelation functions to define 95% confidence levels (Davis, 1976; Kundu, 1976; Sciremammano, 1979). As expected, because the ~ 100 km distance between most of the moorings was of the order of the typical scale of the mesoscale phenomena (50–150 km), and significantly larger than the internal Rossby radius (~ 25 km according to the historical data), the current correlations are generally not significant. From the specific pair 1–1000/2–1000, the most energetic signals have a mean eastward translation speed of ~ 5 km/day. Similar values (3–5 km/day) are obtained from the spectral analysis in the 15–30-day band (not shown), from infra-red imagery, from the specific analysis of "E" (see Section 5), as well as from both theoretical models (Mortier, 1992) and laboratory experiments (Chabert d'Hières *et al.*, 1991) of the Algerian Current mesoscale instabilities. This translation speed is thus definitely the same over the whole depth and appears to be relatively constant.

The temperature correlations are significant for several pairs, mainly at 100 m between points 5, 6, 7 and 8. This is consistent with the fact that the temperature mesoscale variations, being more simple than the current variations, are more similar from place to place. For instance, one can compare the 6–300 and 8–300 records (Fig. 2i,o), which are similar in temperature but different in current.

4.4. *Vertical current structure*

Too many correlation coefficients are significant at 99% (Table 2) to provide reliable information, furthermore as differences on the vertical have previously been evidenced. We consider as significant only the larger coefficients (> 0.9), which are those obtained, with a $\sim 0°$ phase, in the offshore zone (points 5 and 7) between 300, 1000 and 2000 m. They are consistent with the visual analysis of the stick and progressive vector (see Fig. 8) diagrams, as well as with the analysis of the means and variances. Therefore, the deeper structure (at least 300–2000 m) of the mesoscale phenomena is rather barotropic (baroclinic) in the offshore (coastal) zone. This structure can also be characterized in terms of EOF (Kundu and Allen, 1976). At points 1, 3, 6, 7 and 8, where 3–4 relatively long records were available, just 2 modes account for 95–99% of the total energy, with contributions of 85–97% and 2–13% respectively (Fig. 4). At all points except point 3 (due to the relatively long period of south-westward current at 3–1000, which has no fundamental implication), the deep vectors of the first mode make a small angle with the upper one. All deep vectors of the second mode make a relatively wide angle with the upper one and define a zero crossing between 100 and 300 m. The importance of the first mode accounts for fluctuations generally occurring either symetrically or in the direction of the mean surface current. The difference between the barotropic (baroclinic) deeper structure of the phenomena in the offshore (coastal) zone is evidenced by a first mode having more (fewer) parallel vectors, as indicated by points 5, 7 (points 3, 6, 8 and also point 1 which, in this respect, belongs more to the coastal than to the offshore zone).

Table 2. Vertical complex correlations

Point	Depth (m)	Correlation	Rotation (°)	Lag (h)	99% significance level
1	100–300	0.55	−10	0	0.46
	1000–2000	0.69	−7	6	0.39
3	100–1000	0.46	127	−6	0.40
4	1000–2000	0.72	9	−6	0.60
5	100–300	0.54	−19	−12	0.50
	100–1000	0.50	−7	0	0.50
	300–1000	0.94	6	0	0.63
6	100–300	0.43	10	0	0.37
	300–1000	0.44	11	0	0.35
7	300–1000	0.91	10	0	0.63
	300–2000	0.92	−6	−6	0.65
	1000–2000	0.94	3	0	0.63
8	300–1000	0.53	7	−6	0.36
	300–2000	0.35	11	0	0.35
	1000–2000	0.59	10	6	0.39

Only the pairs for which the correlation is greater than the 99% significant level have been reported. A positive rotation is anticlockwise

4.5. *Kinetic energy spectra*

The passage of an eddy-like structure leads to eulerian currents rotating in one or the other sense, so that only total kinetic energy spectra are presented. At 100 m in both zones (Fig. 5a), all spectra show an eddy-containing band from ~20 to 50 days, and relatively low energy at 50–200 days (the minor peak at 5–10 days in the coastal zone cannot be definitely interpreted with the available data). Assuming the 20–50-day phenomena are associated with a ~5 km/day translation speed leads to wavelengths of 100–250 km. At 300 m (Fig. 5b) in the coastal zone, a roughly similar band can be recognized at point 1 as well as, although less clearly, at the other points (3, 6 and 8). On the contrary, the offshore spectra at 300 m display relatively large energy levels at 50–200 days but no specific frequency band. At 1000 m and 2000 m (not shown), features are similar to those at 300 m in the offshore zone and quite erratic in the coastal one.

Therefore, and even if the features at 100 and 300 m are not correlated, wavelengths and periods of 100–250 km and 20–50 days are characteristic of both the coastal (at 100 and 300 m) and the offshore zones (at 100 m only). This similarity of the manifestation of the mesoscale phenomena in the two zones, i.e. independent of the mean circulation, seems paradoxical. In fact, it must first be considered that, because of the wedge-shaped section of the Algerian Current, all these spectra are characteristic of the same surface layer (thicker in the coastal zone than in the offshore one). Second, a phenomenon like "E" will be described in Section 5 as a meander of the Algerian Current (~50 km in width) enclosing a coastal eddy (50–100 km in diameter) while other phenomena, like the open sea eddies "O" in 1986 and "W" in 1984, are 100–200 km in diameter and can be encountered in both zones. The 100-m meters on all moorings, that were located in the surface layer and at less than ~75 km from the coast, are thus actually influenced by the same mesoscale phenomena.

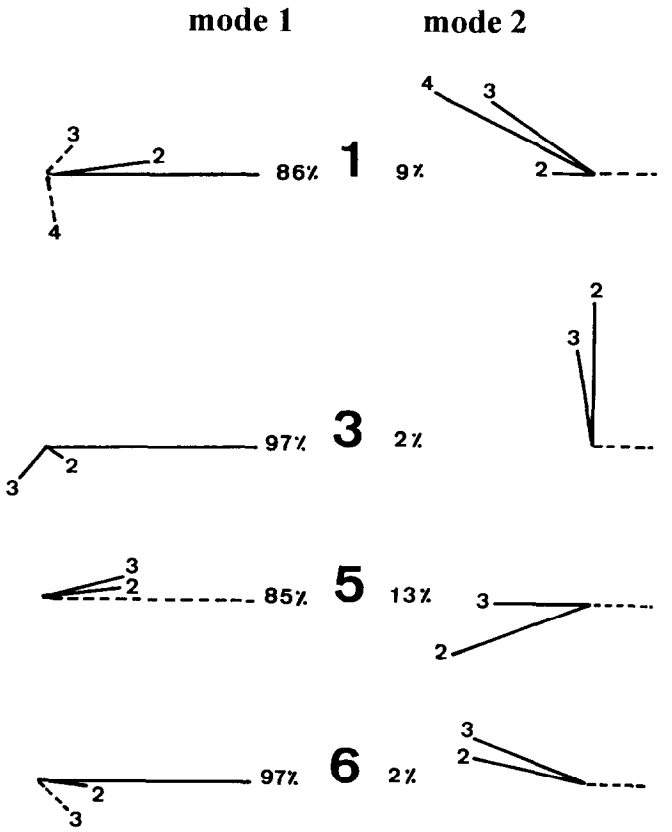

Fig. 4. First (left) and second (right) EOF modes and corresponding energy percentages. The 100 m vectors are normalized and point to the right. The 300, 1000 and 2000 m vectors are identified respectively by 2, 3 and 4. The vector length is proportional to the contribution to the mode. For dashed vectors, direction only is significant.

The similarity of most of the 300 m spectra in the coastal zone and their relatively low amplitude account for the occurrence of mesoscale phenomena neither very intense, nor growing in intensity while propagating eastward. These spectra markedly contrast with those obtained at the same depth (as well as at 1000 and 2000 m) in the offshore zone which have larger energy levels and are associated with longer periods. Now, the longer the period, the lower the translation speed or the larger the size of the phenomena. Assuming a relatively low translation speed at 300–2000 m in the offshore zone would imply that the phenomena there are disconnected from those at 100-m. On the basis of the signatures associated with "E" at point 5, indicating that major changes occur simultaneously at 100 and 300–2000 m, we reject this hypothesis (at least for what concerns "E") and thus concluded that the mesoscale phenomena are relatively energetic and have a relatively large size at depths of 300–2000 m in the offshore zone. As these phenomena can propagate in various directions with various speeds, there is no reason for computing specific periods or wavelengths. At 300–2000 m in the coastal zone, the spectra are much less energetic, which is linked to the location of the moorings mainly on the edge or out of these phenomena.

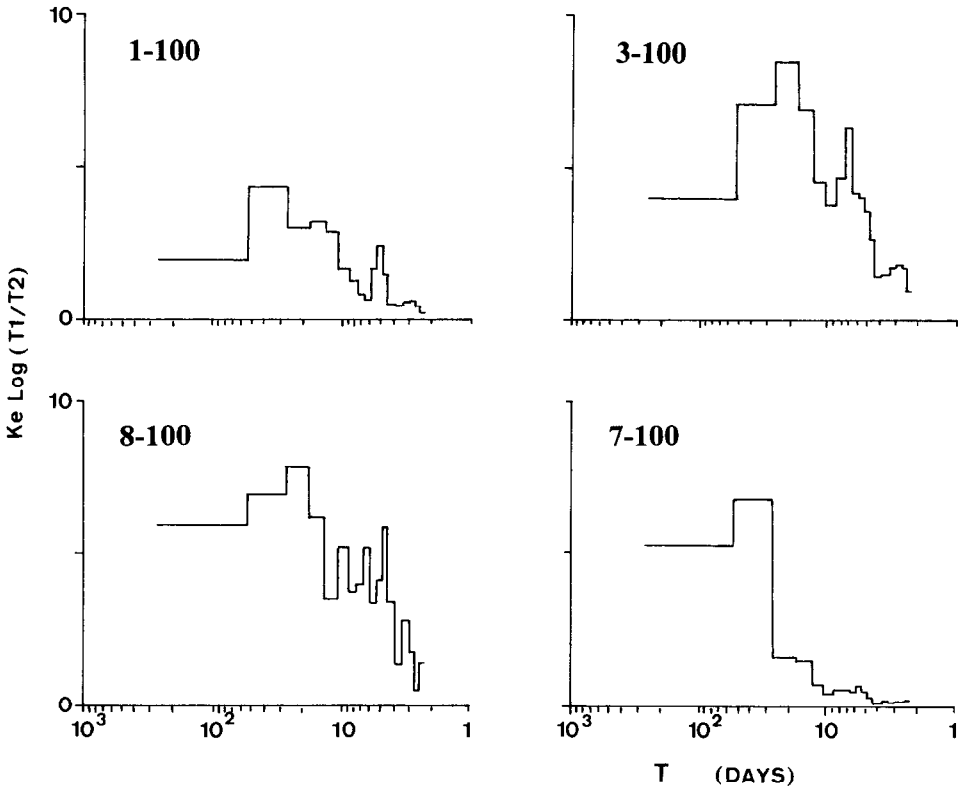

Fig. 5. Kinetic energy spectra in cm^2/s^2 at 100 m (a), and 300 m (b) in the energy-preserving-by-area form (Dickson, 1983) with the 60 lower original frequencies averaged 5 by 5, and the higher 10 by 10.

These basic statistics have suggested several main features which complement the records analysis. In disagreement with our earlier hypotheses, it appears that mesoscale phenomena come rapidly to a mature stage, meaning that their eastward progression is not accompanied by a continuous vertical extension or by a gain in energy. Nevertheless, the space and time scales, as well as the propagation speed and their relatively large intensity, have been confirmed. Mesoscale phenomena appear to be rather similar in the whole surface layer, which is thicker in the coastal zone than in the offshore one. This surface layer is not correlated with the deeper one (> 300 m), even if noticeable mesoscale variations occur at the same time in both layers. Now, in this deeper layer, phenomena in the offshore zone are much more energetic and vertically similar than in the coastal zone. It appears that "E" is a determining feature of the mesoscale variability that needs to be detailed.

5. OTHER ASPECTS OF EVENT "E"

When comparing the infra-red images we have analysed in the past with those collected during this experiment (Fig. 6), event "E" has the classic signature of what we used to call a coastal anticyclonic eddy of moderate-to-large intensity. As a preliminary analysis, let us consider the image on August 21 (Fig. 6a), in which surface isotherms between ~ 1 and 2°E

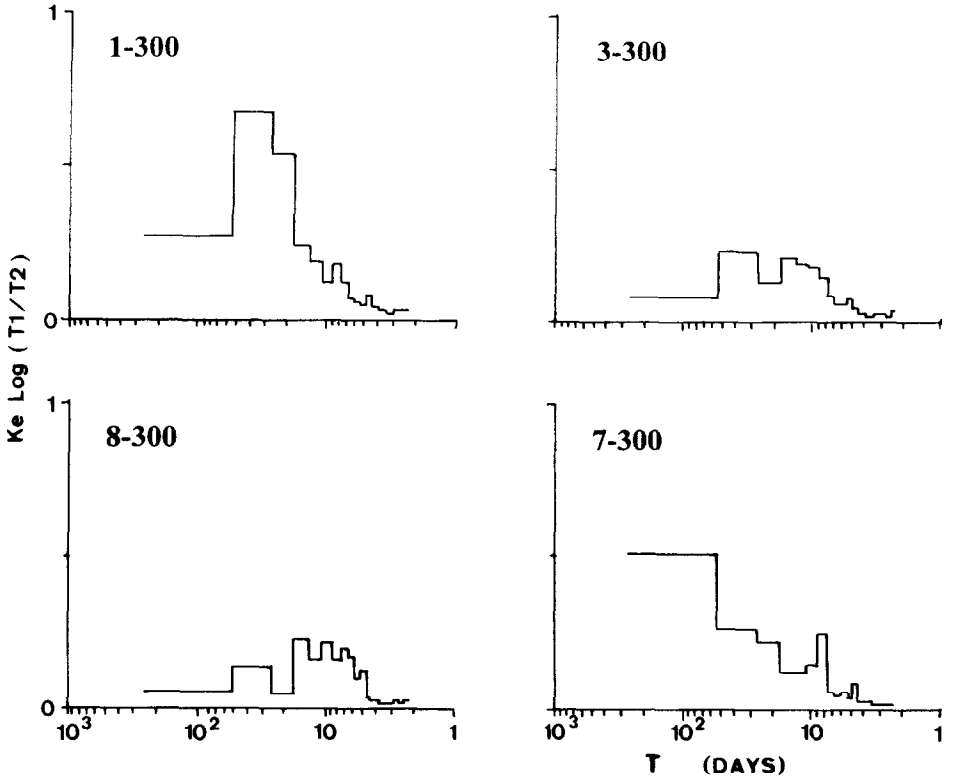

Fig. 5. (*continued*)

and south of ~37°N make "E" looking like a coastal eddy of ~50 km in diameter. It has been checked, during the May–June campaign, that such anticyclonically spiralling isotherms were closely coincident with surface streamlines (Millot *et al.*, 1990). According to geostrophic computations (BMa) and to the fact that the apparent size of such an eddy generally does not continuously increase, it is clear that most of the Algerian Current meanders offshore. "E" has been drifting eastward at ~3 km/day for several months, being characterized by weekly currents at 100 m of several tens of cm/s, in directions which are sometimes perpendicular to the coast for weeks (Fig. 2; Millot, 1991).

The progressive vector diagrams (pvds) obtained at various distances from the coast when an anticyclonic eddy and a surrounding meander proceed slowly (translation speed slower than the current speed) downstream are depicted in Fig. 7. When the mooring is seaward (shoreward) of the eddy centre trajectory, as is point B (point D), the pvd depicts on the right a crenel (loop). When the mooring is close to the centre trajectory as is point C, the pvd shows a turn-back point, while the signature of a meander (point A) and the northern part of an eddy (point B) are similar. Such crenels or loops on the right cannot be due to cyclonic eddies, so that all eddies described in the following are anticyclonic. At the time of crossing, the currents at A, B and D are parallel to the coast, so that actual crossing times are defined by a direction parallel and either in the sense of (crenel) or opposed to (loop) the mean direction of the whole record. The pvds (Fig. 8) are analysed together with the infra-red images, on which currents at 100 and 300 m have been plotted.

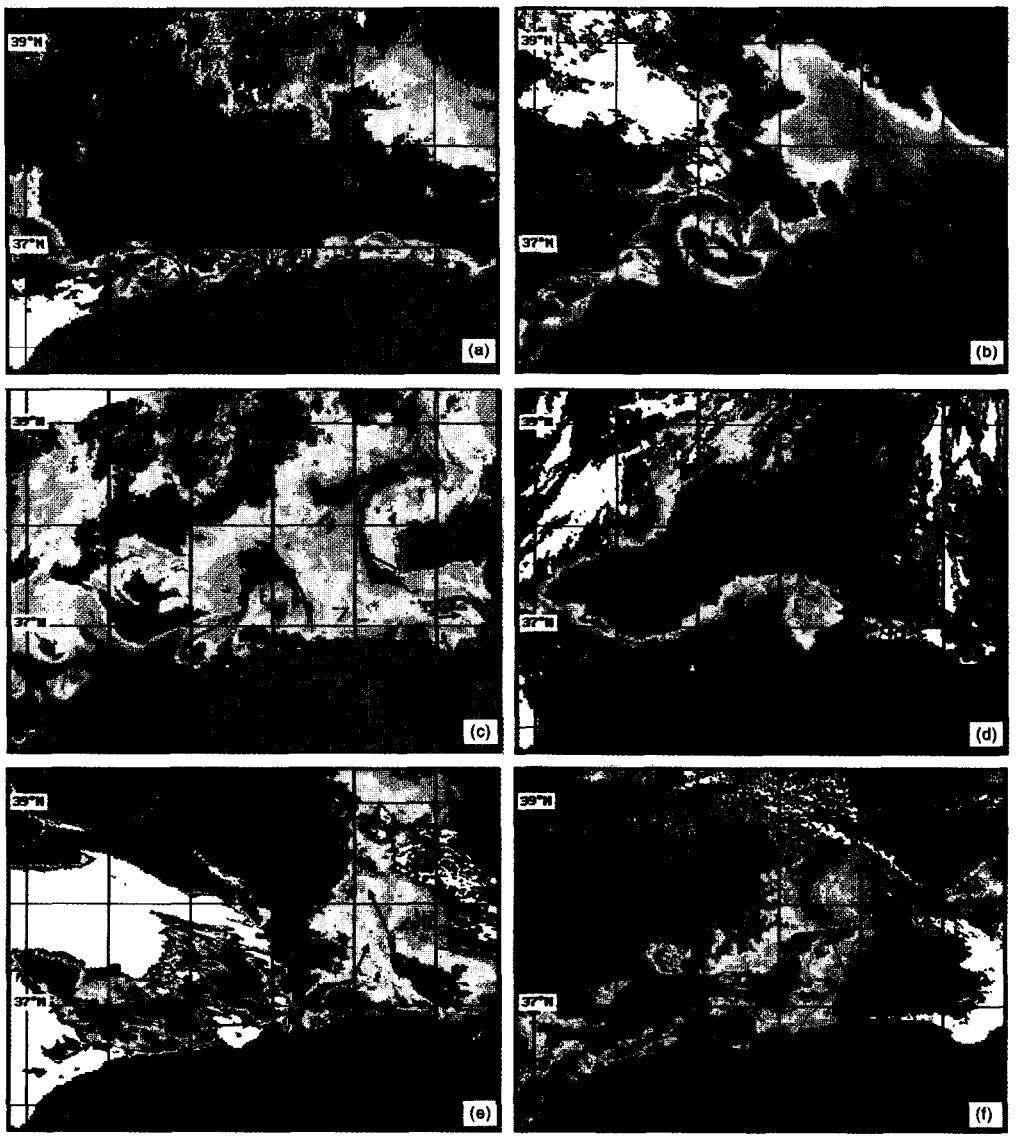

Fig. 6. NOAA/AVHRR sea surface temperature images on August 21 1986 (a), September 5 1986 (b), September 23 1986 (c), October 2 1986 (d), October 22 1986 (e), and November 7 1986 (f). The current vectors are plotted at 100 m (300 m) with full (dashed) line. Speeds lower than 5 cm/s are plotted with arbitrary length; otherwise the vectors are terminated by an arrow. The scale represents 10 cm/s.

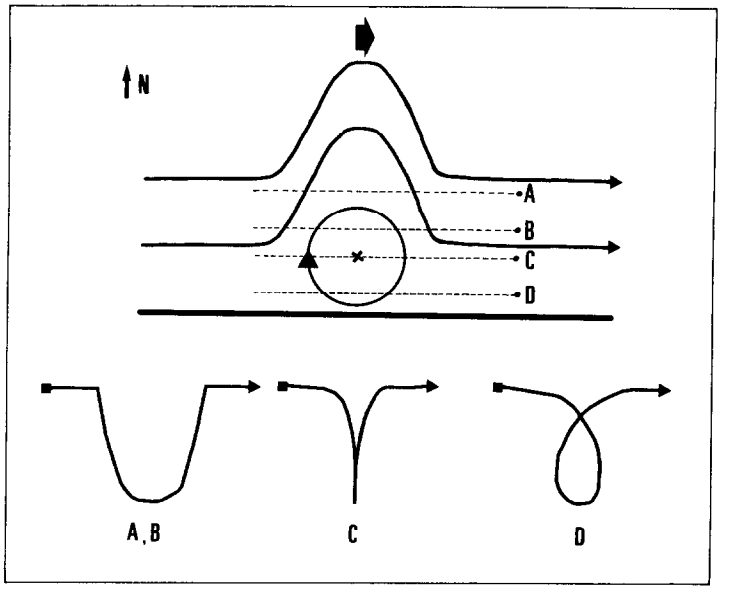

Fig. 7. Schematic progressive vector diagrams obtained when a meander and an anticyclonic eddy slowly propagate eastward over a mooring array.

When in the vicinity of point 1 in late June–early July, "E" is relatively small, not definitely identified on the images and not clearly or simply signed on the current and temperature records. On August 21 (Fig. 6a), the eddy is well developed (diameter ~ 50 km), but the position of its centre with respect to point 3 (in an on–offshore direction) is not clear (point 3 is roughly on the centre trajectory). The 3–100 pvd depicts a crenel and the 3–300 one a loop, while no clear figure is depicted by the 3–1000 pvd (not shown). Such characteristics could be attributed to a unique and twisted eddy, having its axis shoreward from point 3 at 100 m, and seaward at 300 m. But then, the axis has to be dramatically tilted to cross the mooring line between 100 and 300 m, so that such a structure is most unlikely. It could also be interpreted as having basically a two-layer structure associating, in the surface layer, a meander of the Algerian Current surrounding an eddy centred shoreward and superimposed, at depth, on another eddy centred seaward (Fig. 9). In this case, the diameters of the surface and deep eddies can be relatively different, their respective axes vertical, and the inter-axis distance relatively large. In both cases, the deep eddy is not visible at ~ 1000 m at point 3. Such a structure is most likely, as it is typical of baroclinically-generated instabilities (Millot, 1994).

On September 5 (Fig. 6b), the diameter of the surface eddy has increased up to ~ 120 km and its centre is clearly on the north-east of point 3. Therefore, defining the distance between the centre and point 3 when the former passed close to (and to the south of) the latter is difficult. Zooms (not shown) of Fig. 2c,d indicate that the crossing time at 300 m is ~ 1 day earlier than at 100 m (i.e. the deep eddy is ~ 3 km downstream of the surface one); more significantly, they are roughly in phase. Note that "E" influenced point 3 at both 100 and 300 m for ~ 1 month, from early August to early September, which gives a minimum dimension of ~ 100 km for both the meander and the deep eddy.

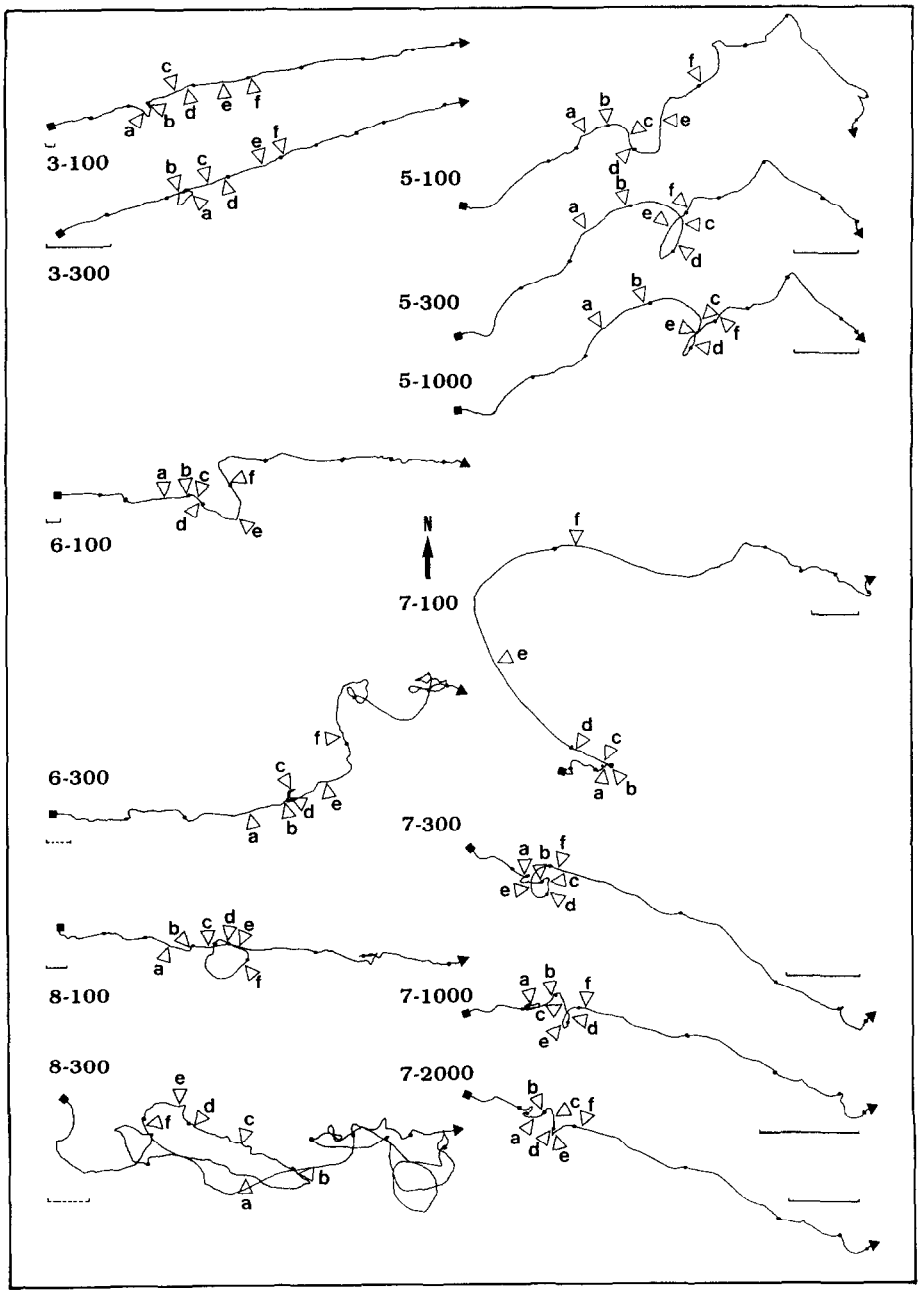

Fig. 8. Some progressive vector diagrams in the coastal (left) and offshore (right) zones. Records begin on June 8 1986 (■), small dots are 30 days apart, letters point at the dates of the infrared images presented in Fig. 6. The full line (dashed line) gives the scale for 100 km (10 km).

On August 21, the 3–100 and 3–300 currents are shoreward (~28 and 10 cm/s) and make a relatively wide angle (~60°), while, on September 5, they are seaward, the speeds still different (35 cm/s vs a few cm/s) and the angle still significant (~30°). In both cases, due to the speed differences and angles, the shear is large, which accounts more for a two-layer structure than for a unique twisted one. In Fig. 6a, the Algerian Current (20–40 km wide) describes a meander whose downstream part is over ~37°N–2°E, around the surface eddy; it is associated with relatively low temperatures so that the classic upwelling is not evidenced. Figure 6b shows that the size of the surface eddy has doubled within two weeks and that a large amount of cool water spirals inside, issued from the upwelling now evidenced. Note that the plume that spreads westward from the northern part of the eddy is a classic feature too, which was followed for several days (images not shown) and which is clearly reproduced by numerical models and laboratory experiments.

Figure 6a,b and Fig. 8 show that, up to early September, no dramatic changes occurred east of ~3°E. But then, up to late October, the 5–100 pvd depicts a crenel, while the 5–300 and 5–1000 pvds depict loops identical in both shape and intensity. Basically, the features are similar to those observed at point 3, but the influence of "E" at point 5 has been longer (~1.5 instead of ~1 month), clearer (well defined at 5–1000, not well defined at 1000 m at points 1, 2 and 3) and more intense (the size of the loop is 150 km at 5–300 and 5–1000 but only 10–30 km at the same depths in the coastal zone). If "E" were merely a twisted eddy, its axis, located south (north) of 5–100 (5–300, 5–1000), should have migrated northward by ~50 km (i.e. from point 3 at ~25 km from the coast to point 5 at ~75 km) to cross the mooring line at point 5, again between 100 and 300 m! This is definitely not satisfying, especially considering Fig. 6c (September 23), which clearly shows that the surface eddy, centred at ~3°E, is still close to the coast (its diameter is 80–100 km). The alternate and satisfying solution is to conclude that a surface eddy, centred at ~50 km from the coast and having the Algerian Current meandering around it, is associated with a relatively intense deep eddy, centred at more than ~75 km offshore. Considering that "E" translated at ~3 km/day, a ~1.5-month influence duration leads to a minimum size of ~150 km for "E", in both the surface (width of the meander) and deep (diameter of the eddy) layers.

The intensity of such deep eddies is also shown by Fig. 2f,g. The 5–300 and 5–1000 daily currents associated with "E" reach values as large as 7–8 cm/s, while the temperature variations at these depths account for a marked subsidence estimated to be 250–300 m at ~1000 m. Two other temperature increases occur at 5–1000 and are associated with more or less intense temperature decreases at 5–300 and current variations at both depths in the form of crenels for several weeks again. As temperature increases at ~1000 m (and temperature decreases at ~300 m) are necessarily due to anticyclonic eddies (the LIW core lies above ~1000 m and the WIW core above ~300 m), it must be assumed that the first one (in late June) translated roughly eastward to the south of point 5 while the second one (in early January) translated westward and also to the south. These signatures cannot be further interpreted, as they can be due either to the same eddy going back and forth or to different eddies passing by.

The characteristics of the "E"-deep eddy at point 5 can be compared with those at points 1 and 3 (Fig. 2). The relatively large temperature decrease at 1–300 and 3–300 is not a proof of large subsidence, as the vertical temperature gradient at ~300 m is larger close to the slope (due to WIW being less modified there) than offshore. At points 1 and 3 this decrease might also be due to an on–offshore displacement of the wedge-shaped edge of the Algerian Current marked by WIW. Now, as the translation speed of "E" was roughly constant, the

relatively short duration (less than 1 month) of its signature at points 1 and 3 accounts either for a relatively small dimension, or for the record of only a part of it. Near point 1 this is probably due mainly to the small dimension of "E". Near point 3 this might rather be due to a deep eddy centred relatively far to the north (point 3 following a chord smaller than a diameter), which is quite probable, as this deep eddy would then be centred north of point 5.

On September 23 (Fig. 6c), the 5–100 and 5–300 currents are south-eastward, so that the surface eddy (80–100 km) and the deep one were centred west of point 5 (more precisely at ~3°E for the former, according to the surface isotherms). Crossing times at 5–300 and 5–1000 are 4–4.5 days earlier than at 5–100 (zooms not shown), so that the deep eddy is actually 15–20 km downstream, but they are considered roughly in phase. A remarkable feature is the direction and increase of the 7–100 current. As supported by the drifting buoy trajectories (Millot, 1991) and the geostrophic and measured currents, this is because most of the Algerian Current surrounded or crossed open sea eddy "O" (sampled in June along its diameter at 4°40′E and appearing on Fig. 6c as the relatively warm feature centred near 38°N–5°E).

On October 2 (Fig. 6d), "E" is still to the west of point 5, it has started to influence 6–100, and the diameter of the surface eddy is ~80 km. The 7–100 current still supports the deflection of the Algerian Current around "O". At the time "E" crosses point 6 (on October 23 at 6–100), the image displayed in Fig. 6e (October 22) reveals a relatively small surface eddy (diameter ~30 km) centred in the south of point 6 and surrounded by the meander, as supported by the crenel shape of the 6–100 pvd (Fig. 8). This image also reveals that the deflection of the Algerian Current toward the north-west becomes more and more sensitive at point 7. But no clear signature of "E" can be seen at 6–300 or at 6–1000 so that, if still existing, the deep eddy associated with "E" must be centred far to the north.

Until mid-October, the translating event "E" and the static eddy "O" were several tens of kilometres away from each other and they did not interact significantly. We know, from the data collected during the May–June campaign, that "O" strongly interacted with the Algerian Current. We have also shown that another coastal eddy, sampled at 4°E (BMa) and having a surface thermal signature similar to that of the "E" surface eddy, disappeared in the cul-de-sac region delineated by "O" and the coast. If "E" is thought to be associating mainly a meander of the Algerian Current ~150 km in width together with a deep eddy ~150 km in diameter and deeper than ~1000 m, then its interaction with eddy "O" (100–150 km in diameter, deeper than ~1000 m) can result only in complex features beyond interpretation with our present data set. As a consequence, some forthcoming analyses, especially those concerning the deep measurements, are more hypothetical than the previous ones. However, interpretation of the 100-m measurements, as it is supported by satellite data, is definitely significant.

The cul-de-sac picture proposed from the May–June campaign to account for the effect of "O" on the surface circulation is well depicted by the 100-m currents. The water flows eastward along the coast at 6–100 and 8–100, turns seaward before reaching ~6°E, and then proceeds north-westward at 7–100, more or less around "O". When "E" is far away from "O", the seaward spreading of the Algerian Current occurs over a wide area, so that its influence over the current at 7–100 is weak. By mid-October, the area is so reduced that there are marked current and temperature increases at 7–100, which account for a relatively thick and intense surface current. Now, a loop is also depicted at depth at point 7, but the marked change of direction occurred only ~4 days later than at point 5, so that these features cannot be due to a unique propagating eddy. The loop at point 7 is less intense and regular

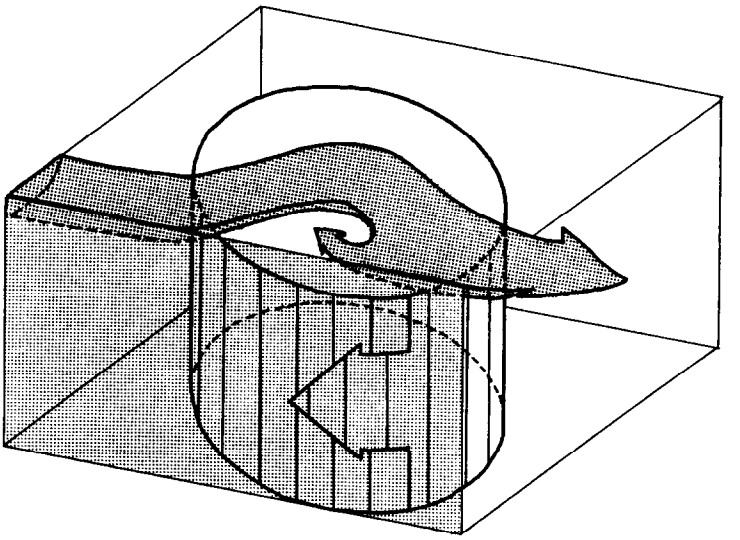

Fig. 9. Schematic 3D diagram of the event "E" structure (from Millot, 1991).

than at point 5 while not being accompanied by a temperature decrease at 7–300. As the change of direction occurs at depth when the 7–100 current intensifies, and as all directions then become similar, we speculate that the loop at depth results more from a local coupling between the surface and deep currents than from the propagation of a mesoscale eddy.

Complementary images were of poor overall quality (cloudiness and seasonal decrease of the recent/older MAW temperature gradient), so that they are schematized in Fig. 10. On October 17 (Fig. 10a), a significant part (if not the whole) of the Algerian Current started again, for the first time since June at least, to flow along the coast east of ~6°E. On November 7 (Fig. 6f), the "E" surface eddy had clearly progressed eastward (centred at ~4°30'E) while its diameter had increased markedly (up to ~120 km, compared to ~30 km two weeks earlier). Consistently, the 6–100 and 7–100 records indicate that the Algerian Current meanders over points 6 and 7 around the surface eddy, while the south-westward direction at 8–100 and the loop of the 8–100 pvd are those expected for a point 8 located as D in Fig. 7. No coherent feature was depicted at 8–300. The area east of ~5°E is cloudy on Fig. 6f, but on the day after (November 8) Fig. 10b shows strong interactions between "E" and "O", and the Algerian Current flowing eastward through the Channel of Sardinia. One month later (December 6, Fig. 10c), point 8 was well within the upstream part of "E" as, after having been north at ~40 cm/s, the 8–100 current is now north-east (~15 cm/s). Owing to cloudiness, no information is available on "O". "E" continued its eastward progression along the coast; it was near 7–8°E by January 6 (Fig. 10d), which is still in agreement with a few km/day translation speed. At that time, the southern limit of "O" was at ~38°N, as if "O" had been pushed seaward by "E".

6. SUMMARY

This paper deals with the analysis of 24 9-month current and temperature time series, collected in 1986–1987 during the Médiprod-5 experiment at depths of 100–2000 m, within

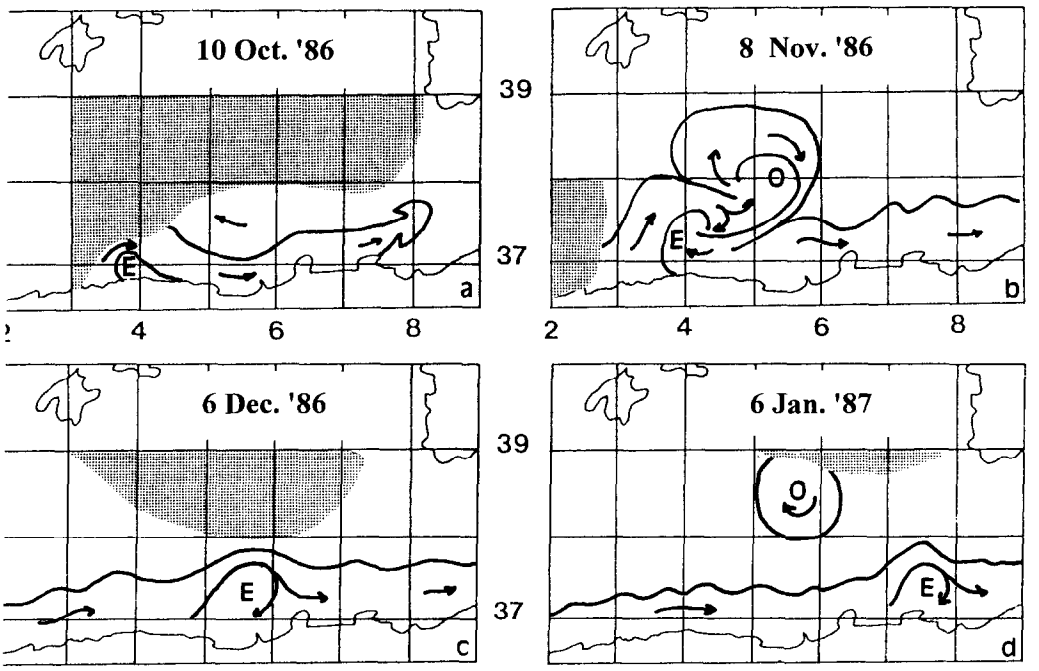

Fig. 10. Main thermal features extracted from NOAA/AVHRR images and schematic interpretation on October 10 1986 (a), November 8 1986 (b), December 6 1986 (c), and January 6 1987 (d).

~75 km of the Algerian coast and between ~0 and 5°E. Statistics allow definition of the hydrodynamical features according to the depth and the distance from the coast: on average, all water masses flow eastward along the slope, while the circulation in the interior of the basin is mainly driven by mesoscale eddies. The paper then focuses on an energetic mesoscale event that crossed the mooring array. To our minds, the structure of an event such as "E" is similar to the one associating, in the atmosphere, the meandering mid-latitude jet and the meteorological systems.

As depicted by pvds, "E" induced a crenel at 100 m at points located at different distances from the coast (~25 km for points 1–3–6 and ~75 km for point 5). "E" must therefore be basically imagined, in most of the MAW layer, as a large meander of the Algerian Current extending seaward for up to several tens of kilometres. As the formation of the meander is associated with negative vorticity, an anticyclonic eddy is rapidly initiated at the surface between the meander and the coast. As long as this surface eddy is centred between the mooring point and the coast, the surface pvd displays a crenel while the loop at 8–100 results from an increase in size of the meander and of the surface eddy it encloses.

As soon as a meander forms, it induces upwelling where it leaves the coast, which allows the surface eddy to be evidenced from infrared images. No doubt the anticyclonically spiralling isotherms observed in the coastal zone, in close coincidence with the intense superficial currents proved by buoys and ship drifts, reflect the actual motions. Now, the apparent diameter of the "E" surface eddy was ~50 km on August 21, ~120 km on September 5, 80–100 km on September 23, ~80 km on October 2, ~30 km on October 22

and ~120 km on November 7. It is thus definitively demonstrated that the diameter of a surface eddy, and the amplitude of the meander around it, display extremely large variations during their eastward course. The surface eddy allows observation from space of mesoscale phenomena looking like "E" but is not their most energetic component.

The clear signature of the relatively deep and large eddy associated with "E" in the offshore zone (large loops at 5–300 and 5–1000) strikingly contrasts with its poor signature at depth in the coastal zone (small loop only at 3–300), although "E" is mainly signed from space in the latter. Considering that "E" propagated eastward at ~3 km/day and influenced point 5 for ~1.5 months gives a rough dimension of ~150 km for both the width of the surface meander and the diameter of the deep eddy. Together with a weak signature at points 3 and 6, which are thus expected to be on the edge, these features are consisent with a deep eddy centred seaward of point 5 at more than ~75 km from the coast. Nevertheless, this deep eddy being large can also be considered as coastal.

The signature of "E" from ~1 to 5°E (i.e. within one half of the Algerian Basin; eastward the features are complicated by the presence of "O") at ~300 m and deeper did not increase along the coast (clear at 3–300 only), while it was clear and barotropic at point 5. Therefore, our previous hypothesis that surface anticyclonic eddies become deeper while progressing eastward is not supported. The Médiprod-5 observations about "E" preferably account for a meander of the Algerian Current rapidly generating (possibly through baroclinic instability) a large eddy at depth, in association with a surface eddy mainly appearing as a consequence (negative vorticity) of the meander. Now, the ability for such a structure to remain coherent during its eastward course strongly depends on the presence of other eddies in the basin. Ultimately, in the Channel of Sardinia, the topography will necessarily decouple the surface flow (which will enter the channel) from the deeper one (which will continue northward), while the surface eddy is generally observed to leave the coast and is expected somehow to merge with the deep eddy.

On the basis of XBT transects (Fuda and Millot, 1995) recently collected from cargo ships between France and Algeria, and with complementary information provided by current meters, ship drifts, infra-red images and Topex-Poseidon altimetric data, we are now able to make more significant relationships between the surface and deep signatures of "E"-like events. We also have proof that, in the eastern Algerian Basin, the surface and deep eddies remain coupled and that, as expected in our circulation diagram, they describe a cyclonic circuit allowing them to trap lenses or entrain patches of the LIW vein around Sardinia and dispatch it to the interior of the Algerian Basin (Fuda *et al.*, in prep.). Even if the structure and generation mechanism of "E"-like events are not fully understood, their links with "open sea eddies" are thus more and more probable.

Another origin for the "open sea eddies" can be proposed, based on models (Käse *et al.*, 1989) and observations (Hinrichsen *et al.*, 1993; Schultz Tokos *et al.*, 1994) showing that Meddies (at 600–1000 m) can entrain the above-lying water. Indeed, laboratory experiments applied to LIW (Baey *et al.*, 1995), with its core at ~300 m, show that the vein can be unstable and generate eddies we call "Leddies" at intermediate depths that can eventually entrain the above-lying water too. Data analysis on hand as well as planned experiments at sea will certainly provide definitive information.

Acknowledgements—This work is a contribution to the EUROMODEL programme supported by DGXII-EC under grant MAST CT 90 00043C. It also received financial and technical support from CNRS/INSU through the GDR "Production Pélagique et Phénomènes Physiques". We wish to acknowledge P. La Violette for organizing

WMCE and who, together with B. Arnone, provided access to NORDA and satellite data facilities, as well as L. Wald, M. Albuisson (ENMP/Sophia Antipolis) and G. Moussu (GM-IMAGE) for help with image processing software. Kind help from F. Schott allowed us to get shiptime from RSMAS/Miami. The CMS team in Lannion, France, as well as the crews of R. V. Le Suroit, Pr. Georges Petit and Columbus Iselin are warmly thanked for their help, as are M. Arhan for fruitful discussions and M. C. Bonin for helping with figures.

REFERENCES

Albérola, C., Rousseau, S., Millot, C., Astraldi, M., Font, J., Garcia-Lafuente, J., Gasparini, G. P., Vangriesheim, A. and Send, U. (1995) Tidal currents in the interior of the Western mediterranean Sea. *Oceanologica Acta*, **18**(2), 273–284.

Albérola, C., Millot, C. and Font, J. (1995) On the seasonnal and mesoscale variabilities of the Northern Current during the PRIMO-0 experiment in the western Mediterranean Sea. *Oceanologica Acta*, **18**(2), 163–192.

Baey, J. M., Renouard, D. and Chabert d'Hieres, G. (1995) Preliminary results about the stability of an intermediate water current. *Deep-Sea Research I*, **42**(11/12), 2063–2073.

Benzohra, M. and Millot, C. (1995) Characteristics and circulation of the surface and intermediate water masses off Algeria. *Deep-Sea Research I*, **42**(2), 1803–1830.

Benzohra, M. and Millot, C. (1995) Hydrodynamics of an open sea Algerian eddy. *Deep-Sea Research I*, **42**(2), 1831–1847.

Brasseur, P., Brankart, J. M. and Beckers, J. M. (1993) *Seasonal Variability of General Circulation Fields in the Mediterranean Sea: Inventory of Climatological Fields*. GHER, University of Liège, Belgium.

Burkov, V. A., Krivosheya, V. G., Ovchinnikov, I. M. and Savin, M. T. (1979) Eddies in the current system of the western Mediterranean Sea. *Oceanologia*, **19**, 9–13.

Chabert d'Hières, G., Didelle, H. and Obaton, D. (1991) A laboratory study of surface boundary currents: Application to the Algerian Current. *Journal of Geophysical Research*, **96**(C7), 539–548.

Conan, P. and Millot, C. (1995) Variability of the northern current off marseilles, western Mediterranean Sea, from February to June 1992. *Oceanologica Acta*, **18**(2), 193–205.

Davis, R. E. (1976) Predictability of sea surface temperature and sea level pressure anomaly of the North Pacific Ocean. *Journal of Physical Oceanography*, **6**, 249 266.

Dickson, R. R. (1983) Global summaries and intercomparisons: flow statistics from long-term current meter moorings. In *Eddies in Marine Sciences*, ed. A. R. Robinson, pp. 278–328. Springer, Berlin.

Fuda, J. L. and Millot, C. (1995) Distribution of the surface and intermediate water masses inferred from the XBT-THETIS 2 transects across the western mediterranean Sea. Rapports Commission internationale de la mer Mediterranée. *CIESM*, **34**, 178.

Guibout, P. (1987) *Atlas hydrologique de la méditerranée*, p. 147. Lab. d'Océanographie Physique du museum, Paris.

Haines, K. and Wu, P. (1996) A modelling study of the thermohaline circulation of the mediterranean. Part 1: water formation and dispersal. *Oceanologica Acta*, **18**(4), 401–417.

Harzallah, A., Cadet, D. and Crépon, M. (1993) Possible forcing effects of net evaporation, atmospheric pressure and transients on water transports in the Mediterranean Sea. *Journal of Geophysical Research*, **98**(C7), 12341–12350.

Herbaut, C., Mortier, L. and Crépon, M. (1996) A sensitivity study of the general circulation of the western Mediterranean Sea. Part 1: the response of density forcing through the straits. *Journal of Physical Oceanography*, **26**, 65–84.

Hinrichsen, H. H., Rhein, M., Käse, R. and Zenk, W. (1993) The Mediterranean water tongue and its chlorofluoromethane signal in the Iberian Basin in early summer 1989. *Journal of Geophysical Research*, **95**(C7), 8405–8412.

Hopkins, T. S. (1988) Recent observations on the intermediate and deep water circulation in the southern Tyrrhenian Sea. "Océanographie pélagique méditerranéenne". *Oceanologica Acta*, **9**, 41–50.

Käse, R. H., Beckman, A. and Hinrichsen, H. H. (1989) Observational evidence of salt lens formation in the Iberian Basin. *Journal of Geophysical Research*, **94**, 4905–4912.

Katz, E. J. (1972) The Levantine Intermediate Water between the strait of Sicily and the Strait of Gibraltar. *Deep-Sea Research*, **19**, 507–520.

Kundu, P. K. (1976) A note on Ekman veering near the ocean bottom. *Journal of Physical Oceanography*, **5**, 238–242.

Kundu, P. K. and Allen, J. S. (1976) Some three-dimensionnal characteristics of low-frequency current fluctuations near the Oregon coast. *Journal of Physical Oceanography*, **6**, 181–199.

Lacombe, H. and Tchernia, P. (1960) Quelques traits généraux de l'hydrologie méditerranéenne. *Cahiers Océanographiques*, **12**(8), 527–547.

Lacombe, H., Tchernia, P. and Gamberoni, L. (1985) Variable bottom water in the Western Mediterranean Basin. *Progress in Oceanography*, **14**, 319–338.

La Violette, P. E. (1990) The western Mediterranean circulation experiment (WMCE): introduction. *Journal of Geophysical Research*, **95**(C2), 1511–1514.

Millot, C. (1985) Some features of the Algerian Current. *Journal of Geophysical Research*, **90**, 7169–7176.

Millot, C. (1987) Circulation in the western Mediterranean Sea. *Oceanologica Acta*, **10**, 143–149.

Millot, C. (1987) The circulation of the Levantine Intermediate Water in the Algerian Basin. *Journal of Geophysical Research*, **92**, 8265–8276.

Millot, C. (1991) Mesoscale and seasonnal variabilities of the circulation in the western Mediterranean. *Dynamics of Atmospheres & Oceans*, **15**, 179–214.

Millot, C. (1994) Models and data: a synergetic approach in the western Mediterranean Sea. *Erice School Proceedings on Ocean Processes in Climate Dynamics: Global and Mediterranean Examples*, eds P. Malanotte-Rizzoli and A. R. Robinson, NATO ASI Series C, Vol. 419, pp. 407–425.

Millot, C. and Bonin, M. C. (1990) Variabilinn té à moyenne échelle du Bassin Algérien. Observations hydrologiques, biologiques et chimiques. Rapport COF N°11, IFREMER, 121 pp.

Millot, C., Taupier-Letage, I. and Benzohra, M. (1990) The Algerian eddies. *Earth-Science Reviews*, **27**, 203–219.

Mortier, L. (1992) Les instabilités d'un courant côtier de densité. Application au Courant Algérien. Thèse de Doctorat de l'Université d'Aix-Marseille II.

Ovchinnikov, I. M. (1966) Circulation in the surface and intermediate layers of the Mediterranean. *Oceanologia*, **6**, 48–59.

Parrilla, G. and Kinder, T. H. (1987) The physical oceanography of the Alboran Sea, report 184, pp. 26. N.O.R.D.A.

Perkins, H. and Pistek, P. (1990) Circulation in the Algerian Basin during June 1986. *Journal of Geophysical Research*, **95**(C2), 1577–1585.

Picco, P. (1990) *Climatological Atlas of the Western Mediterranean*, p. 215. E.N.E.A.

Roussenov, V., Stanev, E., Artale, V. and Pinardi, N. (1995) A seasonal model of the Mediterranean Sea general circulation. *Journal of Geophysical Research*, **100**(C7), 13515–13538.

Sammari, C., Millot, C. and Prieur, L. (1995) Aspects of the seasonnal and mesoscale variabilities of the northern current in the western Mediterranean Sea inferred from the PROLIG-2 and PROS-6 experiments. *Deep-Sea Research*, **42**(6), 893–917.

Schultz Tokos, K. L., Hinrichsen, H. H. and Zenk, W. (1994) Merging and migration of two Meddies. *Journal of Physical Oceanography*, **24**, 2129–2141.

Sciremammano, F. (1979) A note on suggestion for the presentation of correlations and their significance level. *Journal of Physical Oceanography*, **9**, 1273–1276.

Taupier-Letage, I. and Millot, C. (1988) Surface circulation in the Algerian Basin during 1984. "Océanographie pélagique méditerranéenne". *Oceanologica Acta*, **9**, 79–85.